Stationary Potential Patterns during the Reduction of Peroxodisulfate at Ag Ring Electrodes

Peter Grauel, Jan Christoph, Georg Flätgen, and Katharina Krischer*

Fritz-Haber-Institut der Max-Planck-Gesellschaft, Faradayweg 4-6, D-14195 Berlin (Dahlem), Germany

Received: July 1, 1998; In Final Form: October 7, 1998

The potential distribution in front of a Ag ring electrode during the reduction of peroxodisulfate was measured with potential microprobes. Inhomogeneous stationary potential distributions were observed when using a Haber−Luggin capillary, i.e., placing the reference electrode close to the working electrode on the axis of the ring. It is shown that such an arrangement introduces a negative global coupling into the system which destabilizes homogeneous stationary states if the current−potential characteristics exhibits a negative differential resistance. Further consequences of the negative global coupling are discussed, and the effect of an additional, external series resistor is demonstrated.

Introduction

In all disciplines of science much attention has been paid to the spontaneous formation of spatial patterns owing to its importance for the understanding of the emergence of complex structures in nature. In electrochemical systems, the formation of activation waves on passivated iron electrodes was observed long before the theoretical foundation of such self-organization phenomena was laid,[1−5] but only recently a breakthrough in the understanding of the physical mechanisms responsible for pattern formation in electrochemical systems was achieved (for a survey see the review article, ref 6).

In chemical systems, patterns emerge due to the interaction of the dynamics of the homogeneous system, the so-called "local" or "reaction" dynamics, and transport processes, mediating a spatial coupling between different locations of the system.[7,8] In electrochemical systems, the spatial coupling is dominated by migration currents flowing parallel to the electrode.[3,8] The latter are induced by potential patterns that form at the electrode/electrolyte interface. The potential distribution in the electrolyte, and thus also the spatial coupling, depends on the geometry of the electrochemical cell, in particular on the arrangement of working and counter electrode.[11] Furthermore, pattern formation is affected by the operation mode of the system, i.e., whether the voltage between working and reference electrode (potentiostatic control) or the current through the cell (galvanostatic control) is held constant,[12] and as we demonstrate in this paper, also by the relative locations of working, reference, and counter electrodes.

So far, theoretically only cases have been considered where the reference electrode is located on an equipotential plane parallel to the working electrode. The equipotential plane may, e.g., be provided by the counter electrode. If reference and counter electrodes are far away from the working electrode, the change of the state (here the double layer potential) at one position of the electrode affects a whole range of neighboring locations. Hence, in this case the spatial coupling is long-range or nonlocal. This situation was realized also in most experiments carried out under potentiostatic control. A typical feature originating from the nonlocal coupling is the acceleration of waves observed in different experiments.[13,14]

The galvanostatic control introduces an additional global coupling: To keep constant the total current density, a change of the current density at a particular position induces a change of the double layer potential, i.e., a capacitive current, *at every position of the electrode* such that the total current remains constant.[12] It was shown that in this case the global coupling acts synchronizingly, i.e., it acts in a way that local differences in the current density are smoothened out.

Finally, Otterstedt et al. carried out experiments on pattern formation during the anodic dissolution of Co under potentiostatic conditions using an electrode arrangement different from the above-mentioned one: In these experiments the reference electrode was placed close to and in the central position of the working electrode, which was either a disk or a ring electrode.[15] Putting the reference electrode close to the working electrode is an arrangement that is often realized in electrochemical systems as it minimizes the IR drop in the electrolyte between the two electrodes. With this setup Otterstedt et al. observed typically a localized region of high corrosion rate that traveled around the ring or the disk with constant speed. Such a dynamic behavior was not observed during Co dissolution if the reference electrode was at a remote position from the working electrode. Thus, it points to a significant, but up to now not further investigated influence of the position of the reference electrode on the spatial coupling.

In this paper, we investigate pattern formation during the reduction of peroxodisulfate at a Ag electrode in the (or close to) the bistable regime utilizing a setup similar to the one described above: The working electrode is a ring electrode, and the reference electrode is placed close to the working electrode on the axis of the ring. In the result section, it is demonstrated that under such experimental conditions stationary structures form being composed of two domains with different double layer potentials. In the discussion, we derive an equation for the temporal evolution of the double layer potential. From this it becomes apparent that, when putting the reference electrode close to the working electrode, a negative, i.e., *desynchronizing, global coupling* is effective. This type of coupling was also found in other physical or chemical systems,

* Corresponding author. E-mail: Krischer@fhi-berlin.mpg.de. FAX: +49 30 8413 5106.

10.1021/jp982841m CCC: $15.00
Published on Web 11/24/1998

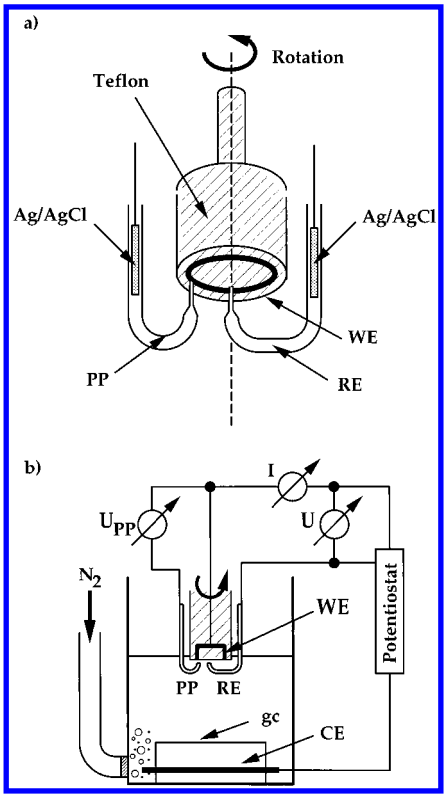

Figure 1. (a) Scheme of the experimental arrangement of reference electrode (RE), potential microprobe (PP), and working electrode (WE), a Ag ring embedded into a Teflon cylinder. The local potential in front of the WE was measured with the PP. (b) Scheme of the complete experimental setup. (gc: glass cylinder.) The potential U between WE and RE was controlled.

such as heterogeneously catalyzed systems[16−22] or dc gas-discharge devices.[23] An explanation for the formation of the stationary patterns is given, following ideas that were originally discussed in connection with the heterogeneously catalyzed systems.

Experiment

The central parts of our experimental setup (Figure 1a) are a rotating Ag ring electrode (the working electrode) and two j-shaped glass tubes which were pulled out to a capillary with an opening of approximately 0.7 mm. One capillary was positioned as exactly as possible on the central axis of the electrode and the other capillary under the ring. Both glass tubes contained Ag/AgCl microelectrodes; the one in the central glass tube served as reference electrode. With the outer one the local potential in front of the working electrode was measured. The working electrode was rotated (in all experiments shown here with 28.5 Hz), thus allowing us to obtain a spatiotemporal picture of the potential distribution in front of the Ag ring. For further experimental details see ref 13.

To guarantee a fast response time, the ends of the capillaries were filled with Na_2SO_4-saturated agar−agar gel over which a 1 M NaCl solution was placed. The distance between the ends of the capillaries and the working electrode was 1 ± 0.2 mm, which proved to be sufficiently far as not to disturb the potential distribution or the transport of $S_2O_8^{2-}$. As can be seen in Figure 1b, the local potential in front of the ring electrode was measured versus the potential of the working electrode. Thus, the measured potential difference is composed of the local double layer potential $\phi_{DL}(x)$ and the potential drop between working electrode and the position of the potential probe. In all plots the quantity shown is the measured voltage minus the externally applied voltage U.

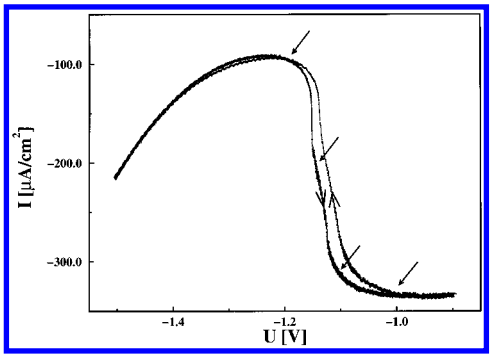

Figure 2. Cyclic voltammogram of a solution containing 0.2 mM $Na_2S_2O_8$ (pH 10, adjusted with NaOH). Sweep rate: 50mV/s. The arrows indicate the potentials at which the stationary measurements shown in Figure 3 were carried out.

The Ag ring electrode (Johnson Matthey, 10 ppm) had an outer diameter of 11.7 mm and a width of 0.75 mm so that the electrode may be viewed as "quasi-one-dimensional", the width being negligible compared to the circumference. Before each experiment the Ag electrodes were polished with 1 μm and 0.25 μm diamond paste, rinsed with acetone pa (pro analysis), ethanol pa, and triply distilled water after each polishing round, and finally treated in triply distilled water in an ultrasonic bath for 10 min. The Pt counter electrode was placed in the main cell compartment remote from the working electrode and bent to a ring to ensure radial symmetry (Figure 1b). It was shielded by a glass cylinder to hinder the reaction products (mainly O_2) from diffusing to the working electrode. N_2 was continuously bubbled through the solution. A potentiostat was used to control the voltage between working electrode and reference electrode. In some experiments a resistance was connected between working electrode and potentiostat. The electrolyte was prepared with triply distilled water and chemicals of pro analysis quality. The glass cell was cleaned with a mixture of concentrated H_2SO_4 and 30% H_2O_2 (3:1) before each experiment.

Results

Figure 2 displays the current−voltage characteristics of a 0.2 mM $S_2O_8^{2-}$ solution. Its most prominent feature is a steep drop in current with increasing overpotential in the region between −1.1 and −1.2 V. Thus, in this region the cyclic voltammogram displays a negative differential resistance (NDR). At potentials anodic of the NDR region, i.e., between the anodic turning point at −0.9 and −1.1 V the current is diffusion limited owing to a high reduction rate. The slow rise of the current negative of the NDR region originates partly from a renewed but weak increase in $S_2O_8^{2-}$ reduction and partly from the beginning H_2 evolution. The overall shape of the diagram is typical for the reduction of an anion or the oxidation of a cation around the point of zero charge (pzc) at low ionic strength. It results from the so-called "Frumkin effects": the variation of the potential within the double layer region and the variation of the reactant concentration at the location of the electron transfer due to electrostatic interaction of reactant and electrode. Positive of the pzc, the concentration of $S_2O_8^{2-}$ is larger than that in the bulk solution due to electrostatic attraction, and negative of the pzc it is smaller due to electrostatic repulsion. It is this "second" Frumkin effect that causes the NDR. In the following we call the reactive states lying anodic to the NDR region "active" and those lying cathodic to it "passive".

In parallel with the current the local potential in front of the ring was measured with the outer potential microprobe. These

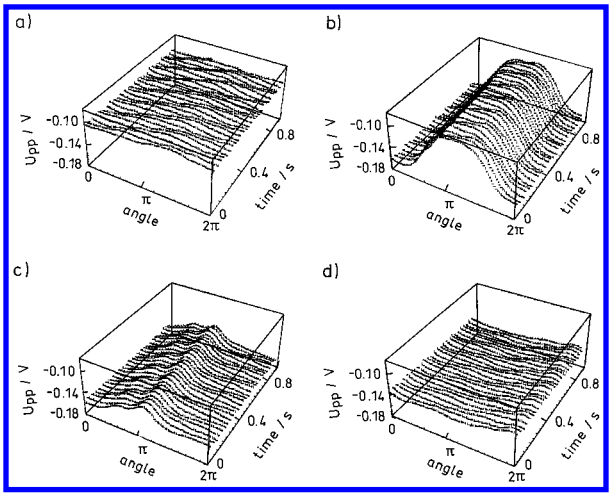

Figure 3. Space-time plot of the local potential measured at four different values of the external potential: (a) −1.2 V, (b) −1.13 V, (c) −1.1 V, (d) −1.0 V (cf. Figure 2).

potential readings revealed that in a part of the voltage region that exhibits the NDR, the potential distribution around the ring was not homogeneous, rather two domains formed, an active domain with the double layer potential anodic to the NDR region and a passive domain with a rather cathodic double layer potential. When holding the external potential at a fixed value within this regime, the domains proved to be stable stationary structures. Four such stationary measurements, recorded at the potentials that are indicated in Figure 2 by arrows, are displayed in Figure 3. Figures 3a and d show angle time plots of the potential probe readings just outside of the NDR region on the passive and the active branch, respectively. Figures 3b and c were recorded at values of U where the current−voltage characteristics possesses a negative differential resistance. These two plots exhibit stationary structures with amplitudes much larger than the potential variations discernible in Figures 3a and d. They reflect a stable nonequilibrium structure that forms at the electrode/electrolyte interface. In contrast, the minor and less regular spatial variations discernible in Figs. 3a and d are to be attributed to inhomogeneities along the ring. The data of Figs. 3b and c are in accordance with the interpretation that in both cases the electrode is split into two domains, an active and a passive one, a narrow, sharp region connecting the two states between: A localized potential structure at the interfaces gradually broadens in the electrolyte with progressive distance from the electrode and decays in amplitude.[13] Thus, at the location of the potential probe the potential pattern is smeared out compared to the one at the electrode.

Regarding the stability of the domains, they lost about 20%−40% in amplitude within a few minutes. The rate of this drift varied somewhat from day to day and most likely results from a slightly changing electrode surface. The latter might be induced by the $S_2O_8^{2-}$ reduction[24] or by H_2 evolution which, to a minor extent, takes place in the passive state. The latter is known to clean the surface and, in particular, to remove bulk oxygen which is dissolved in any silver sample.[25,26] So far, we have not carried out measurements in which we recorded one structure over more than about 5 min. However, this is 3−4 orders of magnitude above characteristic times occurring in the system, such as oscillation period (at different parameters) or current transients when the voltage is changed stepwise. Therefore, we believe that it is justified to classify the observed structures as truly stationary structures in a dynamical sense, i.e., steady state solutions of the underlying evolution equations.

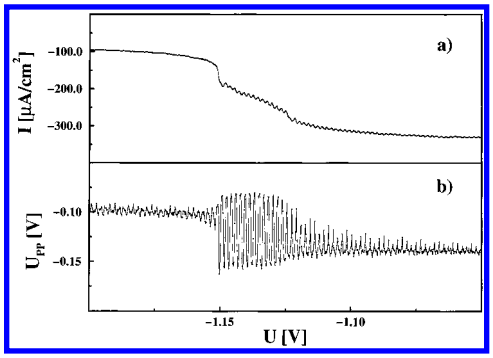

Figure 4. Blowup of the cyclic voltammogram shown in Figure 1 in the transition region between passive and active states during the anodic sweep (a) and corresponding PP measurement of the local potential (vs the reference electrode).

Furthermore, we note that the stationary domains were only easily detectable when coming from the passive region.

Another interesting feature of the stationary structures becomes apparent when we have a closer look at the current in the transition region from the passive to the active branch shown in Figure 2: The rise in the current density occurs in two steps with an only weakly ascending part between (Figure 4a). In the latter "quasi-stationary" current region the local potential exhibits large amplitudes that reach below the passive and above the active branch (Figure 4b). As discussed above, they are to be attributed to two potential domains that form at the electrode/electrolyte interface. Hence, in the region where the spatial domains exist, the current remains "quasi-constant".

The weak oscillations in the current density that are present on the quasi-stationary plateau and also, but with a somewhat smaller amplitude, on the active branch result from a slightly decentric positioning of the reference electrode. The exactly symmetric positioning of the reference electrode turned out to be extremely difficult. Nevertheless, in some measurements we succeeded in positioning the reference electrode sufficiently centric so that hardly any oscillations in the current were discernible. We could not make out any differences in the observed stationary structures between these experiments and those with a slightly asymmetric reference electrode. This fact, together with the explanation of the current oscillations, namely, that the oscillations arise exactly due to the occurrence of spatial structures at the interface (see discussion) makes us confident that the current oscillations do not have any impact on the results presented.

When either increasing the distance between reference electrode and working electrode or inserting a sufficiently large external resistance between working electrode and potentiostat, no stationary structures could be observed anymore, and no state with an intermediate current density between the active and the passive branch could be stabilized. This qualitatively different dynamic behavior is also apparent in the blowup of a cyclic voltammogram (Figure 5b) and the local potential during the passive/active transition plotted as a function of time (Figure 5c). In this experiment the reference electrode was still as close to the working electrode as in the experiments described above, but a 3 kΩ resistor was connected in series to the working electrode. The transition time between the active and the passive state is much faster than in Figure 4, the current density does not increase stepwise, and the local potential exhibits only one "burst" between the active and the passive level. The change in the overall behavior of the cyclic voltammogram can be seen in Figure 5a. Now it exhibits a wide bistable region, as it is

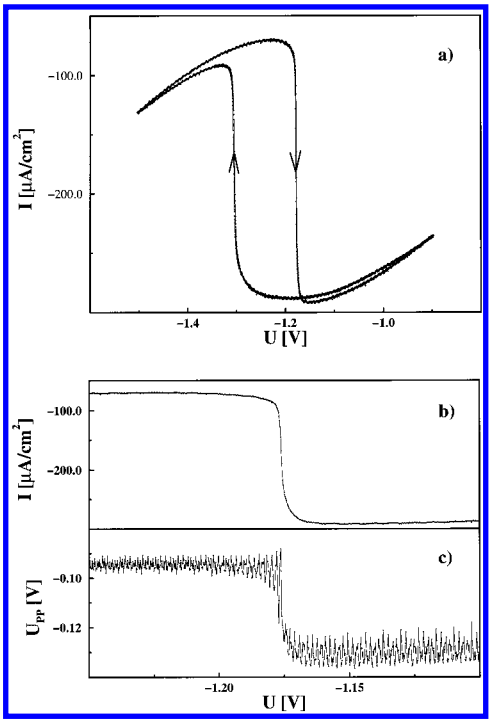

Figure 5. (a) Cyclic voltammogram obtained in a solution containing 0.2 mM $Na_2S_2O_8$ (pH 10) with an external resistor of 3kΩ in series. (Sweep rate: 50mV/s.) (b) Part of the anodic sweep of (a). (c) Corresponding PP measurements of the local potential (vs the reference electrode). Note the different behaviors of current and local potential in this case and in Figure 4.

typical for a system with an N-shaped current/double-layer potential characteristics and a large series resistance.[6,27]

Discussion

The experiments show that stable spatial patterns in the double layer potential form spontaneously in systems with an N-shaped current−potential curve when the reference electrode is placed sufficiently close to the working electrode. The experiments had been guided by theoretical considerations which showed that such an electrode arrangement gives rise to a negative global coupling.[28] In the following we qualitatively derive this finding which explains the formation of the stationary structures. Therefore, we first recall under which conditions a system with an N-shaped current−potential characteristic is bistable. Then we consider how a spatially inhomogeneous double layer potential distribution influences the potential at the location of the reference electrode. Finally, we discuss how this influence feeds back on the double layer dynamics. A quantitative theoretical derivation and simulations will be presented separately.[34]

The emergence of bistability in a homogeneous (lumped) system can best be seen with the help of the equivalent circuit shown in Figure 6a. The parallel connection between the capacitor and the faradaic impedance accounts for two current pathways through the electrode/electrolyte interface: the faradaic and the capacitive currents. The ohmic resistor in series to this interface circuit comprises the electrolyte resistance between working and reference electrode. The voltage drop across both, the interface ϕ_{DL}, and the series resistance is constant, which is in experiments realized by means of a potentiostat. For any stationary state of the system, the faradaic current through the interface $i_{reac}(\phi_{DL})$ is equal to the current through the resistance, which can be expressed as $(U - \phi_{DL})/R_e$, the so-called load line. Thus, the stationary states are intersections of the current−

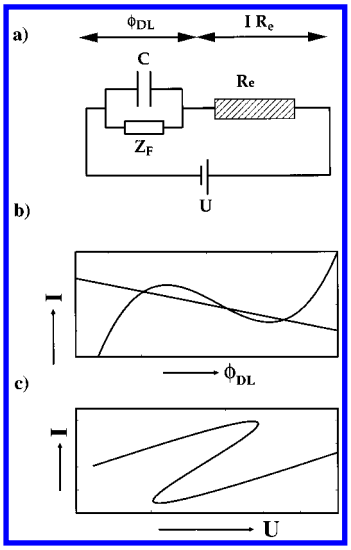

Figure 6. (a) General equivalent circuit of an electrochemical cell with specific double layer capacitance C, faradaic impedance Z_F, electrolyte resistance R_e. (b) N-shaped current−potential curve and load line (see text). The values of U and R were chosen such that the system is bistable. (c) Bistable region in a current vs external voltage plot.

potential characteristics of the interface, which possesses an N-shaped form, and the load line (Figure 6b). For a sufficiently large resistance the two curves possess three intersections. The two outer ones are stable stationary states that are experimentally accessible and lie on the active and the passive branch, respectively, the inner one is unstable. Changing U corresponds to a parallel shift of the load line. Thus, the bistable regime exists in a certain interval of U and manifests itself in a current−voltage measurement in a hysteresis as shown in Figure 6c.

Next, let us consider the influence of a spatially inhomogeneous double layer potential distribution $\phi_{DL}(x)$ on the potential at the location of the reference electrode. A potential pattern at the electrode/electrolyte interface also induces a potential pattern in the electrolyte. In our experiments, this potential pattern exists up to the location of the counter electrode, as the latter provides an equipotential plane parallel to the working electrode. Hence, the potential at the position of the RE, in the following called ϕ_{RE}, does not lie on an equipotential plane parallel to the working electrode. Thus ϕ_{RE} changes if anywhere along the working electrode $\phi_{DL}(x)$ changes locally. For a symmetrically placed reference electrode, the distance between every angular position along the ring electrode and the working electrode is identical. This means that the double layer potential at every angular position along the ring contributes equally to ϕ_{RE} or, in other words, ϕ_{RE} is a function of the *average* double layer potential.

Due to the potentiostatic control condition, a change in ϕ_{RE} is fed back on the temporal evolution of every location of the electrode: Suppose that at some position the double layer potential changes, e.g., due to the formation of an active nucleus in an otherwise passive electrode in the bistable regime. This local transition into the active state changes the potential at the position of the reference electrode, and thus, the iR drop between every point along the working electrode and the reference electrode. However, under potentiostatic conditions the potential difference between working and reference electrode is kept constant, which is achieved by "pumping" charge into the double layer, changing the double layer potential everywhere. Thus, if the reference electrode is not positioned at an equipotential plane parallel to the workig electrode, a change of the state at a particular position is felt instantaneously at every position with

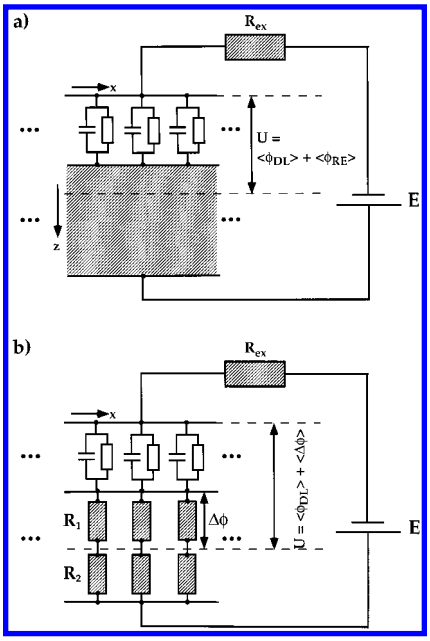

Figure 7. (a) Equivalent circuit for the spatially extended system. The electrolyte is approximated by a two-dimensional cylindrical surface. To capture the dependence of the potential at the location of the reference electrode on the *average* double layer potential in the experiment, the average potential drops across the double layer and the electrolyte up to some distance from the electrode (indicated by the dashed line) is kept constant. (b) Reduced equivalent circuit in which currents parallel to the electrode are "inactivated". R_1 is the "local" resistance at a particular postion x_i between the working electrode and a distance from the working electrode at which the reference eletrode is placed. R_2 is the corresponding resistance between the reference electrode and the counter electrode.

the same strength. Such a coupling is called a global coupling. It is positive if local change and global change have the same sign, i.e., if at one position the system acquires a more anodic potential, the whole system is driven toward more anodic potentials. Correspondingly, the global coupling is negative if a local change toward more anodic values induces a global change toward more cathodic values.

To estimate how the strength of this negative global coupling depends on the distance between working and reference electrodes, we derive equations governing the temporal evolution of the interfacial potential. Therefore, we make use of the equivalent circuit introduced in ref 29 (Figure 7a). The electrode/electrolyte interface is represented by infinitely many, infinitesimally small interface circuits, consisting of the parallel connection between a faradaic impedance and a capacitor. As we are only interested in pattern formation along the circumference of the ring electrode, the interface can be modeled considering only one spatial variable, the azimuthal angle. Furthermore, the calculations are considerably simplified but (as quantitative simulations of the three-dimensional problem show[30]) the qualitative effects are still captured if the electrolyte is confined to a cylindrical surface which is bounded from one side by the working electrode and from the other side by the counter electrode. The latter constitutes an equipotential plane. Because we used in some experiments an external resistor in series to the electrochemical cell, it has been included in the equivalent circuit. In previous papers this equivalent circuit has been analyzed for the case that the reference electrode is at the height of the equipotential plane.[11,12,29] Here we are interested in the dynamic behavior for the instance that the reference electrode is closer to the working electrode than the counter electrode. The fact that in our experiments the potential at the reference electrode is a function of the average double layer potential is taken into account by taking the average electrolyte potential at a given distance from the working electrode and keeping the voltage between working electrode and this averaged potential constant. Thus, all equations derived in ref 29 remain constant with the exception of the equation describing the potentiostatic control which now reads (without external resistor):

$$U = \phi_{DL} + \langle i \rangle R_e \tag{1}$$

where i is the local current through the interface, R_e the resistance between working and reference electrode, and the brackets mean that the average is formed.

To extract the effect of the global coupling, we first consider a hypothetical system in which a current flow parallel to the electrode is prohibited. For instance, one could imagine that there are membranes between working and counter electrode dividing the electrolyte into different compartments and preventing migration currents from one compartment to the other one. In such a case, the equivalent circuit reduces to the one shown in Figure 7b. In each compartment the electrolyte is represented by two resistors R_1 and R_2 which are connected in series between the working and the counter electrode. The average potential drop across R_1 enters the potentiostatic constraint.

When again neglecting the external resistor, a current balance of the reduced equivalent circuit leads to the following evolution equation for double layer potential, ϕ^i_{DL}, in each compartment:

$$C\frac{d\phi^i_{DL}}{dt} = -i_{reac}(\phi^i_{DL}) + \frac{U - \phi^i_{DL}}{R} + \frac{U - \langle \phi^i_{DL} \rangle}{Rr} \tag{2}$$

where i is the compartment number, C is the specific electrode capacitance, $i_{reac}(\phi^i_{DL})$ the faradaic current density, and the three-cornered brackets again mean that the average is taken. R is the resistance between working and counter electrode, and r denotes the ratio of the resistance between working and reference electrode and the resistance between reference and counter electrode; i.e., with the nomenclature of Figure 7b, R and r are defined as

$$R = R_1 + R_2; \quad r = \frac{R_1}{R_2} \tag{3}$$

Obviously, the dynamics of each cell depends on the average double layer potential of all cells. The qualitative effect the average double layer potential has on the dynamics of each cell in eq 2 can be easily rationalized: Suppose that the parameters are such that the electrodes are in the bistable regime and in the active state. If one of the electrodes undergoes a transition into the passive state, which corresponds to larger, i.e., more anodic, values of the positive double layer potential (cf. Figure 6a),[3] the average double layer potential increases which, due to the negative sign in front of $\langle \phi^i_{DL} \rangle$, causes a change of ϕ^i_{DL} toward smaller, i.e., less anodic potentials. In other words, the transition of one electrode into the passive state causes the other electrodes to become more active. Thus, an averaging reference electrode leads to a *negative global coupling*. For a given distance between working and counter electrode, and thus a given resistance R, the global coupling depends only on r: The closer the reference electrode is to the working electrode, i.e., the smaller r, the stronger the global coupling.

When considering the full system, i.e., removing the hypothetical membranes and allowing for cross migration currents in the electrolyte, a current balance at a certain position along

the working electrode leads to the following evolution equation for the double layer potential:[29]

$$C\frac{\partial\phi_{DL}(x)}{\partial t} = -i_{reac}(\phi_{DL}) - \sigma\frac{\partial\phi}{\partial z}|_{z=WE} \qquad (4a)$$

where z is the direction perpendicular to the electrode; $z = WE$, the location of the working electrode; and σ is the specific conductivity of the electrolyte. ϕ is the potential in the electrolyte and $\partial\phi/\partial z|_{z=WE}$ can be calculated from the potential distribution in the electrolyte, which is given by Laplace's equation. If one denotes the distance between working and counter electrode with β and the distance between working and reference electrode with α, the previously defined quantities R and r become σ/β and $\alpha/(\beta-\alpha)$, respectively. Using this notation, eq 4a can be rearranged in the following way:

$$C\frac{\partial\phi_{DL}(x)}{\partial t} = -i_{reac}(\phi_{DL}) + \frac{\sigma}{\beta}(U - \phi_{DL}) + \sigma\left(\frac{1}{\alpha} - \frac{1}{\beta}\right)(U - \langle\phi_{DL}\rangle) + \sigma\left(-\frac{\partial\phi}{\partial z}\Big|_{z=WE} - \frac{1}{\beta}(U - \phi_{DL}) - \left(\frac{1}{\alpha} - \frac{1}{\beta}\right)(U - \langle\phi_{DL}\rangle)\right) \qquad (4b)$$

Here, the second and the third terms on the right-hand side of eq 4b correpond to the latter two terms in eq 2. The additional term, i.e., the last term on the right-hand side of eq 4b, describes the migration cross currents in the electrolyte which are induced by an inhomogeneous potential distribution at the electrode. Hence, this term represents the spatial coupling through the electrolyte and is called the electrolyte coupling term below.

Now we are in a position that we can explain our experimental results, i.e., we can qualitatively answer the questions why and under which conditions we observe stationary domains (Figure 3) and why the current is nearly independent of the externally applied potential if the electrode is in an inhomogeneous state (Figure 4).

We start by reviewing why a negative global coupling leads to stationary domains. This question has been discussed in connection with catalytic reactions where the temperature of the catalyst (in many experiments a "quasi-one-dimensional" wire) was controlled by a constant voltage across the catalyst (wire) which induced an electric current.[16−19,22,31] The evolution equation of the catalyst temperature at a certain location has a structure analogous to eq 4b, i.e., the local change of the temperature is composed of a reaction term, a negative global coupling term that originates from the way the temperature is controlled, and a spatial coupling term arising from heat conductance (which is synchronizing). Hence, the mechanisms for pattern formation are analogous in both systems, and below we transfer the argumentation compiled in ref 8 to our system.

For the moment suppose that the electrolyte coupling term (the last term in eq 4) is much smaller than the global coupling term so that in a first approximation the electrolyte coupling term can be neglected. This is the case if r is much smaller than R, or equivalently $R_1 \ll R_2$. Then also the second term on the right-hand side of eq 4 is much smaller than the third one and can be neglected, and the stationary states, i.e., the solutions of $C(\partial\phi_{DL}/\partial t) = 0$, can be approximated by the following equation:

$$i_{reac}(\phi_{DL}) = \frac{(U - \langle\phi_{DL}\rangle)}{Rr} \qquad (5)$$

Inhomogeneous solutions of eq 5 exist whenever the load line intersects the current potential curve on the branch with the negative differential resistance. Note that this condition is not linked to bistability, though it is obviously fulfilled for the unstable steady state of any bistable system. Furthermore, eq 5 tells us that a stationary pattern of ϕ_{DL} corresponds to a *homogeneous* current density. If we assume that the pattern is composed of active and passive domains, the stationary structure satisfies the following condition:

$$i_{reac}(\phi^a_{DL}) = i_{reac}(\phi^p_{DL}) = \frac{(U - (l\phi^a_{DL} + (1 - l)\phi^p_{DL}))}{Rr} \qquad (6)$$

Here the length of the electrode is normalized to 1, and l denotes the portion of the electrode that is in the active state. ϕ^a_{DL} and ϕ^p_{DL} are the double layer potential of the active and the passive branch, respectively. Note that this condition is satisfied by any arbitrary distribution of active and passive states, as long as the sum over the active and the passive region equals l and $(1 - l)$, respectively. However, this is not the only degeneracy in the system. As soon as there exists an inhomogeneous solution with a given current density, and thus also a given value of l, there exist inhomogeneous solutions for all other current densities in the multivalued region of the current density curve, each current density being realized by a different ratio of active and passive areas, i.e., a different value of l.

Next let us investigate how the picture changes if the electrolyte coupling is taken into account. The argumentation becomes more illustrative if we assume that the system is bistable and the homogeneous active and passive states coexist with the stationary potential pattern. If one prepares an inhomogeneous state that satisfies eq 5 with an arbitrary current density within the multivalued current interval, the inhomogeneous potential distribution induces migration currents parallel to the electrode which drive the system into the more stable of the two stationary states. For example, for an inhomogeneous state with a reaction current close to the low-current border below which only the homogeneous active state exists (I_1 in Figure 8a), the active state is the more stable one, and thus, this one would expand on the expense of the passive one. Now suppose that the electrolyte coupling is very weak compared to the global coupling. Then the decreasing average double layer potential (cf. eq 3) leads to an increase of ϕ^a_{DL} and ϕ^p_{DL}, and thus also of the average current density. This means that the system is driven into the bistable regime, the active state becoming less stable and the passive one more stable until both states are equally stable and the front velocity becomes zero. This situation is indicated by I_{cr} in Figure 8a. An analogous argument holds for an initially inhomogeneous situation in which the passive state is the more stable one: While the passive state expands, ϕ^p_{DL} becomes smaller, and the state is again driven toward I_{cr}. Thus, in the case of very weak electrolyte coupling, one of the possible inhomogeneous solutions of eq 5 is selected, namely, the one for which both steady states of the bistable regime are equally stable.

A change of a parameter, e.g., U, does not affect the local current density of an inhomogeneous steady state, but the relative portions of the active and the passive state change such that the stationary state condition is still satisfied. Within the existence region of the inhomogeneous solution, l, i.e., the ratio between active and passive state, changes between 0 and 1, and the system behaves smoothly in I and ϕ_{DL} at the transition points between inhomogeneous and homogeneous solutions (Figure 8). In other words, in the limit of the vanishing electrolyte coupling the negative global coupling acts like a current stabilizer. This effect was observed for the heterogeneously

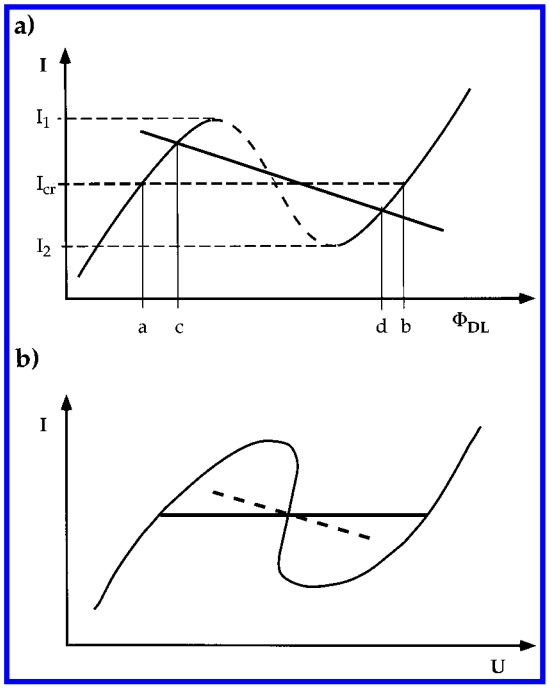

Figure 8. (a) Schematic current−potential curve illustrating the values of the double layer potential and current in the inhomogeneous states in the limit of vanishing electrolyte coupling: The current density always corresponds to I_{cr} at which the two states are equally stable. For comparison, the load line is shown for a certain electrolyte resistance. It is evident that active and passive potentials in the inhomogeneous states (a and b) are always further apart than those of two homogeneous states (c and d) in the bistable region. (b) Schematic current−voltage characteristics illustrating the existence region of inhomogeneous states for weak electrolyte coupling (thick solid curve) and stronger electrolyte coupling (thick dashed curve).

catalyzed systems and is utilized in a technical device called "barretter".[32]

A gradual increase of the electrolyte coupling reduces the parameter interval in which the inhomogeneous states exist and leads to small deviations in the current density of ϕ_{DL}^{a} and ϕ_{DL}^{p} in the inhomogeneous stationary state, as indicated in Figure 8b (dashed line). Thus, for intermediate values of the electrolyte coupling there is a jump in the total current density at the transition point between the homogeneous and inhomogeneous solutions. This is exactly the behavior we observed experimentally (cf. Figure 4).

Experimentally, no stationary domains could be detected when an external resistor with a sufficiently large resistance was connected in series to the cell. In ref 12 it is shown that the external series resistor gives rise to a *positive global coupling*, thus counteracting the negative global coupling as well as the formation of patterns. The interplay between the two global couplings can be quantified for the equivalent circuit shown in Figure 7. Defining the parameter $g = R_{ex}/R_2$, the third term on the right-hand side in eq 2 reads

$$\frac{U - \langle \phi_{DL}^{i} \rangle}{R(r+g)}(1-g) \qquad (3)$$

Thus, as long as $g < 1$, the external resistor weakens the negative global coupling, for $g = 1$ it exactly compensates it, while for $g > 1$ the global coupling becomes positive.

Finally, we can explain the origin of the superimposed oscillations on the current trace in Figure 4: Above it was argued that the potential on the axis of the ring is a function of the average double layer potential along the ring. As a consequence of a tiny deviation from the central position, the potential at the location of the reference electrode is not exactly the average potential any more but a weighted average. Hence, an inhomogeneous potential distribution along the ring together with the rotation of the electrode lead to an oscillating potential at the reference electrode. The potentiostat keeps this potential constant by changing the potential at the counter electrode which results in the observed current oscillations. Thus, they represent an imperfection of the experiments. However, according to the above arguments, it can be excluded that they cause the formation of the stationary domains. Rather, patterns at the electrode bring about the current oscillations.

Last of all, it should be mentioned that Otterstedt et al. found antiphase behavior during the anodic oxidation of a Co ring when they placed the reference electrode close to the center of the ring, i.e., points on opposite sides of the ring exhibited anticorrelated dynamics.[33] It is very likely that these phenomena are another manifestation of the negative global coupling that is induced by the position of the reference electrode.[34] This conjecture is supported by experiments and simulations of heterogeneously catalyzed, nonisothermal reactions with negative global coupling where antiphase oscillations were observed as well in the oscillatory region of the reaction.[21,35,36]

Concluding Remarks

The investigations demonstrate how important it is to incorporate the spatial variable in model considerations about the dynamics on electrode reactions. Especially if stationary the patterns form, as in the case considered here, the occurrence of a dynamic instability will not be obvious from measurements of a global quantity, such as the electrode potential or the average current density, which may lead to pitfalls in the interpretations of experimental data. These considerations point to the necessity of enhancing our knowledge about spatiotemporal pattern formation in electrochemical systems and, thus, of performing spatially resolved measurements. However, therefore the development of further instrumental techniques for the in-situ investigation of the *local* potential, current density or concentration seems to be necessary. Up to now, only three methods were employed for local measurements, micro potential probes, visible light microscopy and surface plasmon microscopy.[37] Each of these methods underlies certain restrictions concerning the systems that can be studied.

Acknowledgment. We are grateful to G. Ertl for his steady support and thank M. Eiswirth for fruitful discussions. P.G. gratefully acknowledges a "Kekulé" grant from Fonds der chemischen Industrie.

References and Notes

(1) Heathcote, H. L. *Z. Phys. Chem.* **1901**, *37*, 368.
(2) Lillie, R. S. *Science* **1918**, *48*, 51.
(3) Bonhoeffer, K. F.; Renneberg, W. *Z. Phys.* **1941**, *118*, 389.
(4) Bonhoeffer, K. F. *Z. Elektrochem.* **1941**, *47*, 147.
(5) Franck, U. F. *Z. Elektrochem.* **1951**, *55*, 154.
(6) Krischer, K. In *Modern Aspects of Electrochemistry*; *vol. 32*, Conway, B. E., Bockris, J. O., White, R., Eds.; Plenum: New York, 1998.
(7) Murray, J. D. *Mathematical Biology*; Springer: Berlin, 1990.
(8) Mikhailov, A. S. *Foundations of Synergetics I*, 2nd ed.; Springer: Berlin, 1994.
(9) Krastev, I.; Baumgartner, M. E.; Raub, C. J. *Metalloberflaeche.* **1992**, *46*, 116.
(10) Krastev, I.; Koper, M. T. M. *Phys. A* **1995**, *213*, 199.
(11) Mazouz, N.; Flätgen, G.; Krischer, K. *Phys. Rev. E* **1997**, *55*, 2260.
(12) Mazouz, N.; Flätgen, G.; Krischer, K.; Kevrekidis, I. G. *J. Electrochem. Soc.* **1998**, *145*, 2404.
(13) Flätgen, G.; Krischer, K. *Phys. Rev. E* **1995**, *51*, 3997.

(14) Otterstedt, R.; Plath, P. J.; Jaeger, N. I.; Sayer, J. C.; Hudson, J. L. *Chem. Eng. Sci*. **1996**, *51*, 1747.
(15) Otterstedt, R. D.; Plath, P. J.; Jaeger, N. I.; Hudson, J. L. *J. Chem. Soc., Faraday Trans*. **1996**, *92*, 2933.
(16) Zhukov, S. A.; Barelko, V. V. *Sov. J. Chem. Phys*. **1982**, *4*, 883.
(17) Volodin, Y. E.; Barelko, V. V.; Merzhanov, A. G. *Sov. J. Chem. Phys*. **1982**, *5*, 1146.
(18) Philippou, G.; Luss, D. *Chem. Eng. Sci*. **1993**, *48*, 2313.
(19) Luss, D. *Phys. A* **1992**, *188*, 68.
(20) Middya, U.; Graham, M. D.; Luss, D.; Sheintuch, M. *Phys. D* **1993**, *63*, 393.
(21) Middya, U.; Graham, M. D.; Luss, D.; Sheintuch, M. *J. Chem. Phys.* **1993**, *98*, 2823.
(22) Liauw, M. A.; Somani, M.; Annamalai, J.; Luss, D. *AIChE J*. **1997**, *43*, 1519.
(23) Willebrand, H.; Hüntler, T.; Niedernostheide, F. J.; Dohmen, R.; Purwins, H.-G. *Phys. Rev. A* **1992**, *45*, 8766.
(24) Flätgen, G.; Krischer, K.; Ertl, G. *J. Electroanal. Chem.* **1996**, *409*, 183.
(25) Zemlyanov, D. Y.; Savinova, E.; Scheybal, A.; Doblhofer, K.; Schlögl, R. Preprint, 1998.
(26) Schlögl, R. Private communication.
(27) Koper, M. T. M. *Adv. Chem. Phys*. **1996**, *92*, 161.
(28) Christoph, J. Internal report, 1997.
(29) Flätgen, G.; Krischer, K. *J. Chem. Phys.* **1995**, *103*, 5428.
(30) Christoph, J. Unpublished results.
(31) Middya, U.; Luss, D. *J. Chem. Phys*. **1994**, *100*, 3568.
(32) Barelko, V. V.; Beibutyan, V. M.; Volodin, Y. V.; Zeldovich, Y. B. *Dokl. Akad. Nauk SSSR* **1981**, *257*, 339.
(33) Otterstedt, R. Ph.D. Thesis, Universität Bremen, 1997.
(34) Christoph, J.; et al. Manuscript in preparation.
(35) Cordonier, G. A.; Schmidt, L. D. *Chem. Eng. Sci.* **1989**, *44*, 1983.
(36) Graham, M. D.; Lane, S. L.; Luss, D. *J. Phys. Chem*. **1993**, *97*, 7564.
(37) Flätgen, G.; Krischer, K.; Pettinger, B.; Doblhofer, K.; Junkes, H.; Ertl, G. *Science* **1995**, *269*, 668.
(38) An exception hereof is the Ag/Sb deposition where convection seems to be resoponsible for the pattern formation observed.[9,10]
(39) Figure 6 is shown for positive currents (oxidation reactions) i.e., the overpotential increases when going toward more positive double layer potentials. In the case of reduction reactions, the signs of current density and double layer potential have to be reversed. Thus, in that case, the passive branch is more negative, and a higher total current leads to a more negative double layer potential, and thus, again to a “more passive” electrode.